Impact of subsurface crevassing on the depth-age relationship of high-alpine ice cores extracted at Col du Dôme between 1994 and 2012

Susanne Preunkert[1], Pascal Bohleber[2,3,4] Michel Legrand[1,5], Hubertus Fischer[6], Adrien Gilbert[1], Tobias Erhardt[6,7], Roland Purtschert[6], Lars Zipf[2,8], Astrid Waldner[2], Joseph R. McConnell[9]

[1]Université Grenoble Alpes, CNRS, Institut des Géosciences de l'Environnement (IGE), Grenoble, France
[2]Institute of Environmental Physics, Heidelberg University, Heidelberg, Germany
[3]Institute for Interdisciplinary Mountain Research, Austrian Academy of Sciences, Innsbruck, Austria
[4]Ca' Foscari University of Venice, Department of Environmental Sciences, Informatics and Statistics, Scientific Campus, via Torino 155, 30172 Mestre (VE), Italy
[5]Laboratoire Interuniversitaire des Systèmes Atmosphériques, Université de Paris and Univ Paris Est Creteil, CNRS, LISA, F-75013, France
[6]Climate and Environmental Physics, Physics Institute, and Oeschger Centre for Climate Change Research, University of Bern, Switzerland
[7]Alfred Wegener Institute, Helmholtz Centre for Polar and Marine Research, Bremerhaven, Germany
[8]Laboratoire de Glaciologie, Université Libre de Bruxelles, Brussels, Belgium
[9]Division of Hydrologic Sciences, Desert Research Institute, Reno, Nevada, USA

Correspondence to: Susanne Preunkert (suzanne.preunkert@univ-grenoble-alpes.fr)

Abstract.

Three seasonally resolved ice-core records covering the 20th century were extracted in 1994, 2004 and 2012 at a nearly identical location from the Col du Dôme (4250 m above sea level, m asl, Mont Blanc, French Alps) drill site. Here we complete and combine chemical records of major ions and radiometric measurements of ^3H and ^{210}Pb obtained from these three cores together with a 3D ice flow model of the Col du Dôme glacier to investigate in detail the origin of the discontinuities observed in the depth-age relation of the ice cores drilled in 2004 and 2012. Taking advantage of the granitic bedrock at Col du Dôme, which makes the ice core ^{210}Pb ice-core records sensitive to the presence of upstream crevasses, and the fact that the depth-age disturbances are observed at depths for which absolute time markers are available, we draw an overall picture of a dynamic crevasse formation. This can explain the non-disturbed depth-age relation of the ice core drilled in 1994 as well as the perturbations observed in those drilled in 2004 and 2012. Since crevasses are common at high alpine glacier sites, our study points out the mandatory need for rigorous investigations of the depth-age scale before using high alpine ice cores to interpret atmospheric changes.

1. Introduction

35

Close proximity to European source regions makes ice cores from high-elevation Alpine glaciers an important target to reconstruct past anthropogenic perturbations of atmospheric chemistry. In the French Alps, the Col du Dôme (CDD) glacier close to the Mont Blanc summit has been studied extensively over the last 25 years for its glaciological properties and suitability for glacio-chemical studies (e.g. Vincent et al., 1997, Preunkert et al., 2000). The glacier has been shown to be

40 entirely cold although it has experienced a significant warming in response to climate change since the 1980s (Vincent et al., 2007; Gilbert and Vincent, 2013; Vincent et al., 2020). Ice cores extracted at CDD have been used to reconstruct various aspects of atmospheric changes during the 20th century over western Europe. These include major inorganic species (NH_4^+, NO_3^-, and SO_4^{2-}, Fagerli et al., 2007, Preunkert et al., 2003, and Preunkert et al., 2001a), halogens (HCl and HF, Legrand et al., 2002, Preunkert et al., 2001b; total I and Br, Legrand et al., 2018 and Legrand et al., 2021), black carbon (Moseid et al.,

45 2022), dissolved organic carbon (DOC, Legrand et al., 2013), organic molecules (Legrand et al., 2003 and 2007, Guillermet et al., 2013), and trace elements such as Pb and Cd (Legrand et al., 2020), V and Mo (Arienzo et al., 2021), and Tl (Legrand et al., 2022). Underpinning these efforts are three ice cores all drilled to bedrock within maximal 10 m of each other (mean geographic location of 45.842195° N, 6.84675° E) in 1994 (C10, Vincent et al., 1997, Preunkert et al., 2000), 2004 (CDK, Legrand et al., 2013) and 2012 (CDM, Legrand et al., 2018, this study).

50 Whereas analysis of the C10 ice core drilled in 1994 indicated a depth-age relationship that was consistent between the derived annual layer counting and several time markers (Preunkert et al., 2000), it was shown that the 2004 CDK core was missing ~ 16 years between ~ 1970 and ~ 1954 (Legrand et al., 2013) as confirmed by the absence of the well-known ^{3}H maximum in 1963 caused by atmospheric nuclear tests. Although its precise cause remained unclear, it was suggested that the missing 1954-1970 period was related to an (upstream) crevasse that had disturbed the continuity of the CDK record through inflow of a

55 snow filled crevasse to the ice core site. The presence of one or more crevasses in the upstream vicinity of the drill site was also suspected to cause strongly elevated concentrations of ^{210}Pb observed in the C10 core (Vincent et al., 1997). This was concluded, since the bedrock at the CDD consists of granite that emits ^{222}Rn (half-life of 3.8 days), which is able to diffuse in snow and firn, but much less in ice (see also Pourchet et al., 2000), and subsequently decays to produce ^{210}Pb (half-life of 22.3 years).

60 For the CDM core, only the upper core sections (down to 81 m depth, i.e. 1979) have been investigated previously for various trace elements including major ions, black carbon, halogens, Pb, Cd, V and Mo, Tl (Legrand et al., 2018, 2020, 2021, 2022, Arienzo et al., 2021, Moseid et al., 2022, Eichler et al., 2022). Here we report additional measurements of the ^{210}Pb profile and use NO_3^-, NH_4^+ and ^{3}H analysis, to extend the depth-age relationship of the CDM core back to 1950. This homogeneous set of chemical and radiochemical data from the C10, CDK and CDM ice cores, permits to investigate the consistency of the depth-

65 age relation back to 1950 between these ice cores drilled in 1994, 2004, and 2012. In addition, a first attempt to provide a qualitative glaciological explanation for the observed discontinuity in the depth-age relation and the link with the presence of

unexpectedly high ^{210}Pb levels will be made. This is important for understanding of the extent to which existing and future ice cores drilled at this location on the CDD saddle are suitable to reconstruct past atmospheric chemistry changes.

2. Site and Analysis

70 The CDD site is located on a small cold glacier saddle downslope of the Dôme du Gouter (4300 m asl) (Fig. 1). On this slope, the C10, CDK, and CDM cores were drilled down to ~125 m (Table 1), i.e., close to bedrock. Detailed glaciological descriptions of this site can be found in Vincent et al. (1997, 2020), whereas Preunkert et al. (2000) characterized this site in terms of its usefulness to reconstruct past atmospheric changes since the beginning of the 20th century based specifically on data from the C10 ice core. Ice flow, firn compaction and thermal regime have been modeled in three dimensions by Gilbert

75 et al. (2014), allowing particle back-tracking and flow-based estimation of the depth-age relationship for the drilling site.
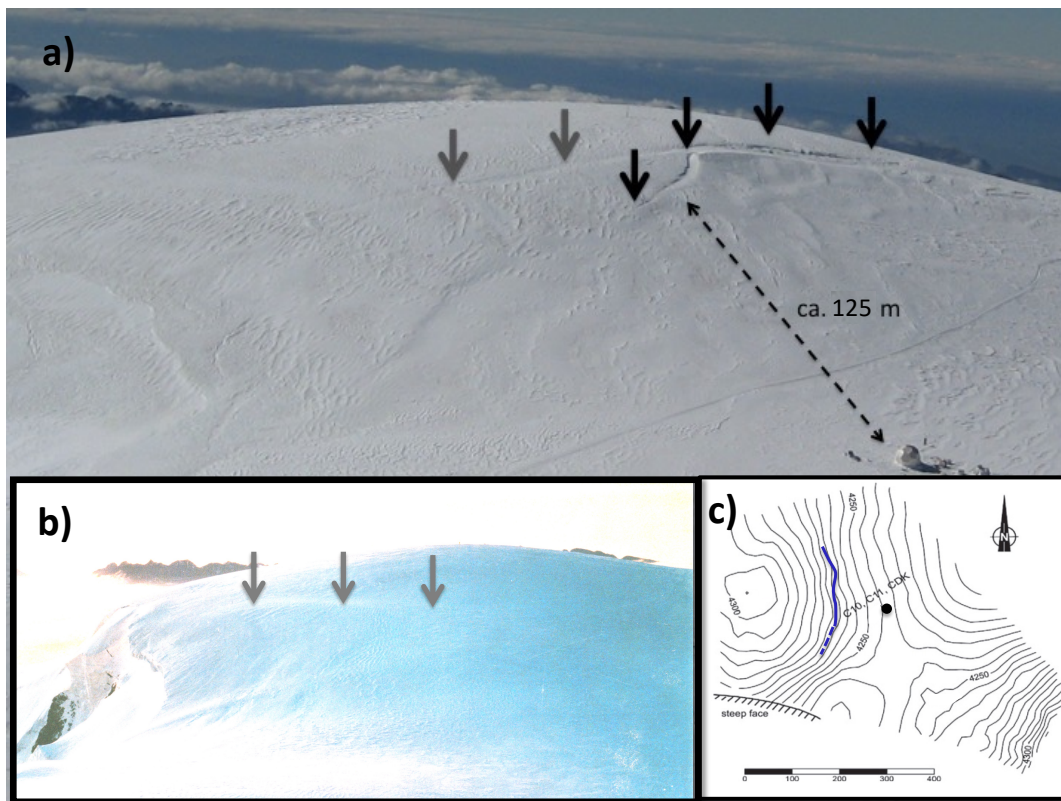
Figure 1: View of the South-East flank of the Dome de Gouter (CDG) and Col du Dome saddle including the drill site of 1994, 2004,
80 **and 2012 situated downslope of Dome du Gouter. (a) Picture taken in summer 2012: A large crevasse extends across the upstream catchment area (indicated with black arrows) of the drilling site. At that time the distinctly visible crevasse was mainly snow-covered. A potential second crevasse is indicated by grey arrows. (b) Picture taken in summer 1999: Evidence of a crevasse limited to the southwestern side of the Dome du Gouter. (c) Topographic map of the Col du Dome and Dome de Gouter (adapted from Wagenbach et al. 2012). The crevasse highlighted in (a) and (b) is reported (blue line in (c)) on the base of an aerial photo from Institut national**
85 **de l'information géographique et forestière (IGNF) taken at 30th June 2004. Contour lines are spaced at 5 m interval.**

Recent visual observations made on the CDD glacier attest to the presence of crevasse(s) upstream the CDD drill sites (Fig. 1). Comparing photos taken in 2012 (Fig. 1a) and in 1999 (Fig.1b), shows an enlargement and horizontal propagation of the crevasse to the east from 1999 to 2012. Whereas in 2012, the crevasse is visible clearly as a snow-covered depression on the surface slope, the crevasse appeared to be limited to the southwestern flank of the drill site catchment area in 1999.
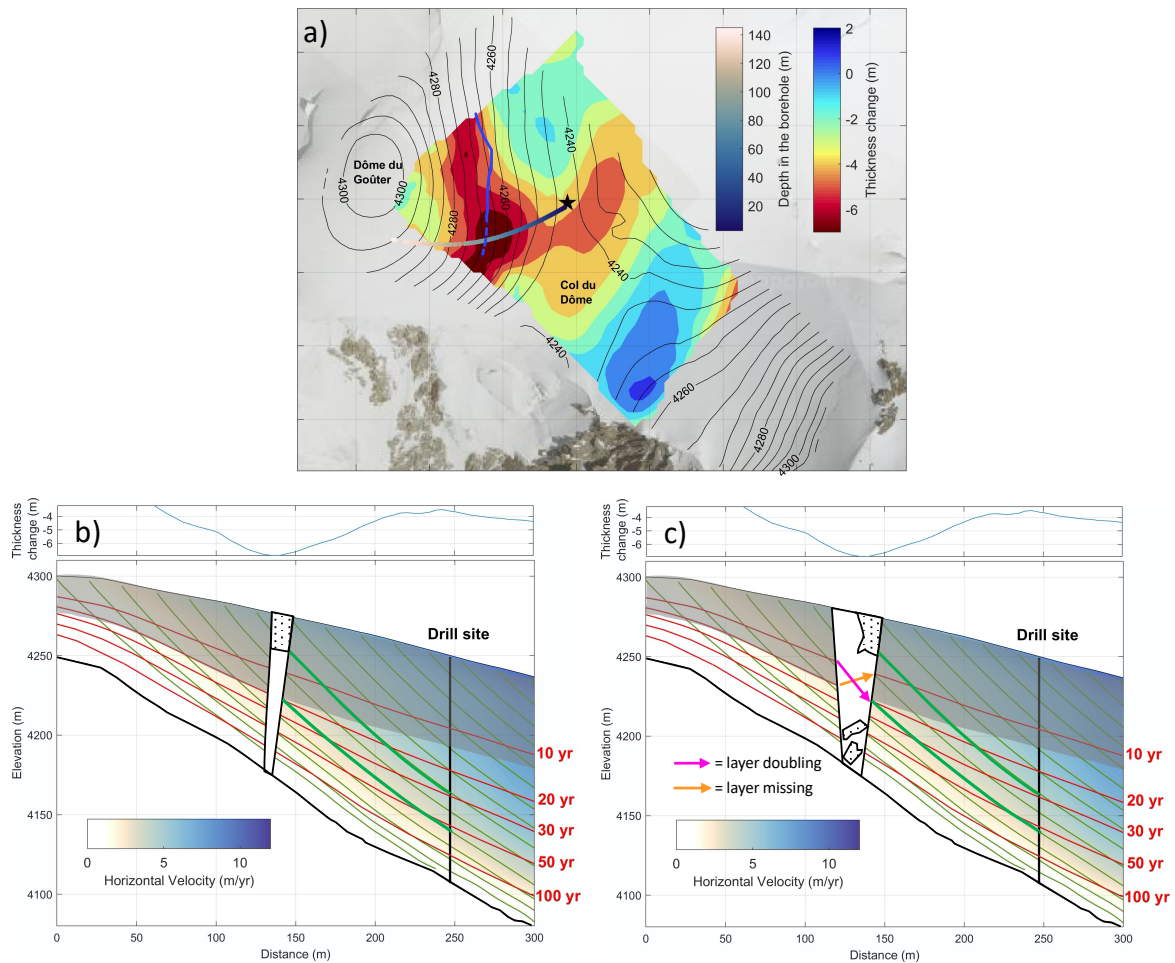

Figure 2: (a) Thickness changes between 1993 and 2017. The contour lines of surface topography correspond to the 1993 surface (adapted from Vincent et al., 2020) overlain by a modelled flow line (color scale on top) which reports the calculated arrival depth at the drill site of C10, CDK, and CDM (black star) (Gilbert et al., 2014). The crevasse location (blue line) is based on the 30th June 2004 aerial photo from IGNF (see Fig.1) (b and c) Schematic representation of the origin of the 210Pb anomalies found at the drill site following the ice flow model of Gilbert et al., 2014, extracted along the flow path reaching the drill site. Isochrones are marked in red, flowlines in green (see also Section 4). The grey shaded zone indicates firn, the dotted zone indicates the snow bridge over the crevasse. Concluded from ice core data of C10, CDK and CDM (see Section 3 and 4), two states of the crevasse are reported: (b) in the years ~1965-1970 (i.e. ~ 25-30 years before the C10 drilling) the crevasse is open to the bedrock but sealed from the atmosphere by a snow bridge. In this state 222Rn and 210Pb accumulate to reach concentrations well above atmospheric conditions in the crevasse and the surrounding firn (c) after ~1975 and at least until ~1990 (i.e. ~ 25-30 years before the CDK and CDM drilling), the crevasse is at least partly open to the atmosphere. In this state 222Rn and 210Pb concentrations in the crevasse and the surrounding firn are strongly reduced compared to (b). The formation of missing or doubling ice layers is indicated by the orange and pink arrows.

4

105 Following Fig. 1, the crevasse is situated ~100-150 m upstream of the drill site of C10, CDK, and CDM. Figure 2a shows the CDD glacier thickness changes between 1993 and 2017 overlayed with the modelled flow line indicating the calculated arrival depths at the drill site of C10, CDK, and CDM (Gilbert et al., 2014). Crevasses are known to open and close constantly during their lifecycle (Colgan et al., 2016). Fig. 2b and c represent vertical cross sections along the modelled flow line of Fig. 2a overlayed by sketches of the upstream crevasse visible in Fig.1, in two temporal states of the crevasse from the 1960ties to the

110 1980ties, as concluded in Section 4 of this manuscript on the basis of C10, CDK and CDM ice core data presented in Section 3.

Table 1 summarizes the main characteristics of the three ice cores and basic findings related to radiometric analyses. ^{3}H analyses in CDK (Legrand et al., 2013) and CDM ice were performed at the Institute for Environmental Physics, Heidelberg University (IUP), by low-level gas counting with a detection limit typically around 1.5 TU (tritium units). ^{210}Pb samples of

115 CDK and CDM ice were analyzed at IUP by α-spectrometry for its decay product ^{210}Po. Typical blank values of (5.7 ± 2.5) 10^{-5} Bq for ^{210}Po and (3.8 ± 1.6) 10^{-5} Bq for ^{209}Po were subtracted from the sample counts (see Stanzick, 2001, and Elsässer et al., 2011 for further working analytical conditions). Previously reported ^{210}Pb measurements in C10 ice (Vincent et al. 1997) analyzed at the Laboratoire de Glaciologie et Géophysique de l'Environnement, now Institut des Géosciences de l'Environnement (IGE), were complemented by two samples. The analytical technique was high-resolution gamma-ray

120 spectrometry, designed to detect very low levels of radioactivity using a 20% high-purity Ge (N-type) detector, with an anti-Compton scintillation detector (Pinglot and Pourchet,1995) for which snow and ice samples were filtered previously through ion-exchange papers (Delmas and Pourchet,1977). This method is less sensitive than α-spectrometry and Vincent et al. (1997) did not assign uncertainties to their analyses. Here we estimate the uncertainty based on what has been reported in other studies using this detection method developed at IGE. Pinglot et al., 2003 reported a detection level of 10 mBq at a 97.5% confidence

125 level for 3 days of counting on ice core samples with a typical ^{210}Pb activity of 20 – 50 mBq kg^{-1}. These measurements included Chernobyl fallout in sub-Arctic glacier sites, and the levels were similar in range to the background activities of 50-100 mBq kg^{-1} found in our cores. On the other hand, detection levels of 13 and 25 mBq were calculated at 97.5 % confidence when peak interferences where neglected or considered, respectively, for a 10 g sediment sample containing 1000 times higher ^{210}Pb activities as found in ice cores (~70 Bq kg^{-1}) that was measured for 63 hours (Pinglot and Pourchet, 1995). Vimeux et al.

130 (2008) reported a lower detection limit of 4 mBq kg^{-1} for ^{210}Pb measurements (activities between 20 and 100 mBq kg^{-1}) on relatively small (150-250 g) ice core samples from Patagonia. The ^{210}Pb activities in C10 ranged from 50 – 700 mBq kg^{-1}, with the measurements done on the C10 drilling chips merged over 3 to 5 m, allowing to obtain sample weights of up to ~ 3 to 5 kg. Since these sample masses, type (ice core sample) and geometry (filter) are comparable to those used in the Pinglot et al. (2003) study but are very different from the sediment sample in Pinglot and Pourchet (1995), we assume in the following a

135 detection level of 10 mBq and an uncertainty of 30 mBq for the C10 ^{210}Pb measurements. Note that, the dataset from Vincent et al. (1997) was complemented by two additional samples for which ^{210}Pb analysis and quality control were not available in 1997. Initially suspected to be contaminated, these two samples, containing 760 and 460 mBq kg^{-1} of ^{210}Pb, were not included reported by Vincent et al., 1997. Re-measurements of the respective ice core sections using samples extracted from the inner

140

^{3}H analyses (using liquid scintillation counting) in CDM ice were also performed at the Division for Climate and
Environmental Physics (CEP) of the Physics Institute, University of Bern, using ice core samples at higher depth resolution
than used at IUP.

Continuous flow analyses in the CDM core, including nitrate (NO_3^-) and ammonium (NH_4^+), were made at Desert Research

145 Institute (DRI) in Reno from 45 to 86 m depth (see Legrand et al. (2018) and references therein). Additional NO_3^- and NH_4^+
data that are useful to derive an age scale by annual layer counting at CDD (Preunkert et al., 2000) were obtained in CDM ice
with CFA measurements conducted at CEP along the whole ice core.

150 **Table 1: Basic glaciological and radiometric parameters of the CDD ice.**

Core name	C10	CDK	CDM
Drilling year	1994	2004	2012
Ice core length [m]	126	124	122.5
Surface (uppermost 15years) accumulation [m (mwe)]	6 (2.6)	3.8 (2.5)	3.5 (2.3)
Accumulation over uppermost 30 years [m (mwe)]	2.9 (2.1)	2.7 (2.0)	2.6 (1.85)
Firn-ice transition [m (years)]	56 (13)	54 (14)	52 (14)
Depth of the ^{3}H maximum [m]	87.67	-	93.3 (87.3)
Top and bottom depth of the ^{210}Pb anomaly [m]	83–108	85—~108	81-~102

Working conditions of the CFA analyses at CEP are detailed in Kaufmann et al. (2008), Gfeller et al. (2014) and Erhardt et al
(2022). However, since the CDM ice core has a 3 inch diameter, the ice core cross section available for the CFA analyses at
CEP was only a section of 2.5 x 3.0 cm instead of the usual standard size of 3.2 x 3.2 cm used at CEP, for which the standard

155 melt head is designed for. This may have led to a higher risk of contamination of the inner sample melt water stream and
implied a reduced analyte spectrum. Despite the undersized core section available for the CFA analyses at CEP, 86% of the
ice core could be analyzed. The nitrate profile obtained at DRI and CEP (covering 97% in this depth range), were compared
from 45 to 86 m depth. Both datasets are in very good agreement. After having additionally discarded very high peaks in NO_3^-
values (1.5% of CEP data), which were not present in the DRI dataset and could be attributed easily to contamination, mean

160 NO_3^- values from 45.3-86.0 m were 263 ppb (CEP) and 255 ppb (DRI) (Fig. 3). The agreement is somewhat weaker for NH_4^+
likely because only 80% of the depth range is covered by the CEP measurements. After discarding additionally 8 % of the

CEP NH$_4^+$ data consisting of high NH$_4^+$ peaks which were not present in the DRI dataset, the mean NH$_4^+$ values of 101 ppb (CEP) and 95 ppb (DRI) were in good agreement.

## 3. Data and Methods

3.1 Ice Core Dating

The net annual accumulation in the upper layers of the site covering the upper 15 years is on average 2.5 m water equivalent (mwe) (Table 1), a typical order of magnitude encountered at high alpine glacier sites (Vincent et al., 2020; Bohleber, 2019). The surface mass balance observed in the upstream area of the drilling site (i.e., upwind in the southeastern Dôme du Gouter flank, Fig.1) decreases by one order of magnitude and reaches only ~0.2 mwe yr^{-1} at the summit of the Dôme de Gouter (Vincent et al., 1997, 2020), where the glacier thickness is only ~40 - 45 m. In addition to the annual layer thinning caused by the glacier flow, this upstream net accumulation decrease which is accompanied by a decrease of the winter to summer net snow accumulation rate, also impacts the annual layer thickness at the drill site. As a consequence, annual layer thicknesses of only 0.7 and 0.2 mwe are observed at 100 m and 118 m depth (Preunkert et al., 2000) and the winter to summer layer thickness ratio, calculated on the basis of the ammonium depth stratigraphy (see details in Preunkert et al., 2000), decreases from 1 at the surface to 0.5 at 100m depth.

Based on the well-marked seasonality in the chemical stratigraphy for all cores, annual layer counting was used as the main dating tool over the time period of interest in this study. This was supplemented by Saharan dust events such as the one in 1977 (Preunkert et al., 2000 for C10; Legrand et al., 2013 for CDK, Legrand et al., 2018 and this study for CDM) and radiometric analyses aimed at detecting fallout from atmospheric thermonuclear bomb testing via ^{3}H (Legrand et al., 2013 for CDK and this study for CDM) and ^{137}Cs (Vincent et al., 1997) for C10, as already done for other Alpine ice cores records (e.g. Schotterer et al., 1998). Fallout from atmospheric thermonuclear bomb testing typically leads to elevated ^{137}Cs and ^{3}H levels from 1954 to about 1975, with maxima in 1963 if the depth-age relationship is well preserved. The ^{210}Pb depth profiles (Vincent et al., 1997 for C10) were also obtained in the three ice cores, but because of the presence of the strong anomalies discussed in Section 3.2, these data are not useful as dating tools.

3.1.1 The C10 core

The dating of the C10 ice core back to 1925 obtained from annual layer counting of the ammonium record was initially established by Preunkert et al. (2000). More recently, the availability of additional measurements such as lead, cadmium and thallium allowed the dating to be extended back to 1890 without changing the original dating back to 1935 (Legrand et al., 2018).

The agreement between results of the annual layer counting and several time markers shows that the depth-age relation is continuous and increases monotonically with depth (Fig. 3). The dating of the C10 core was found to be in excellent agreement
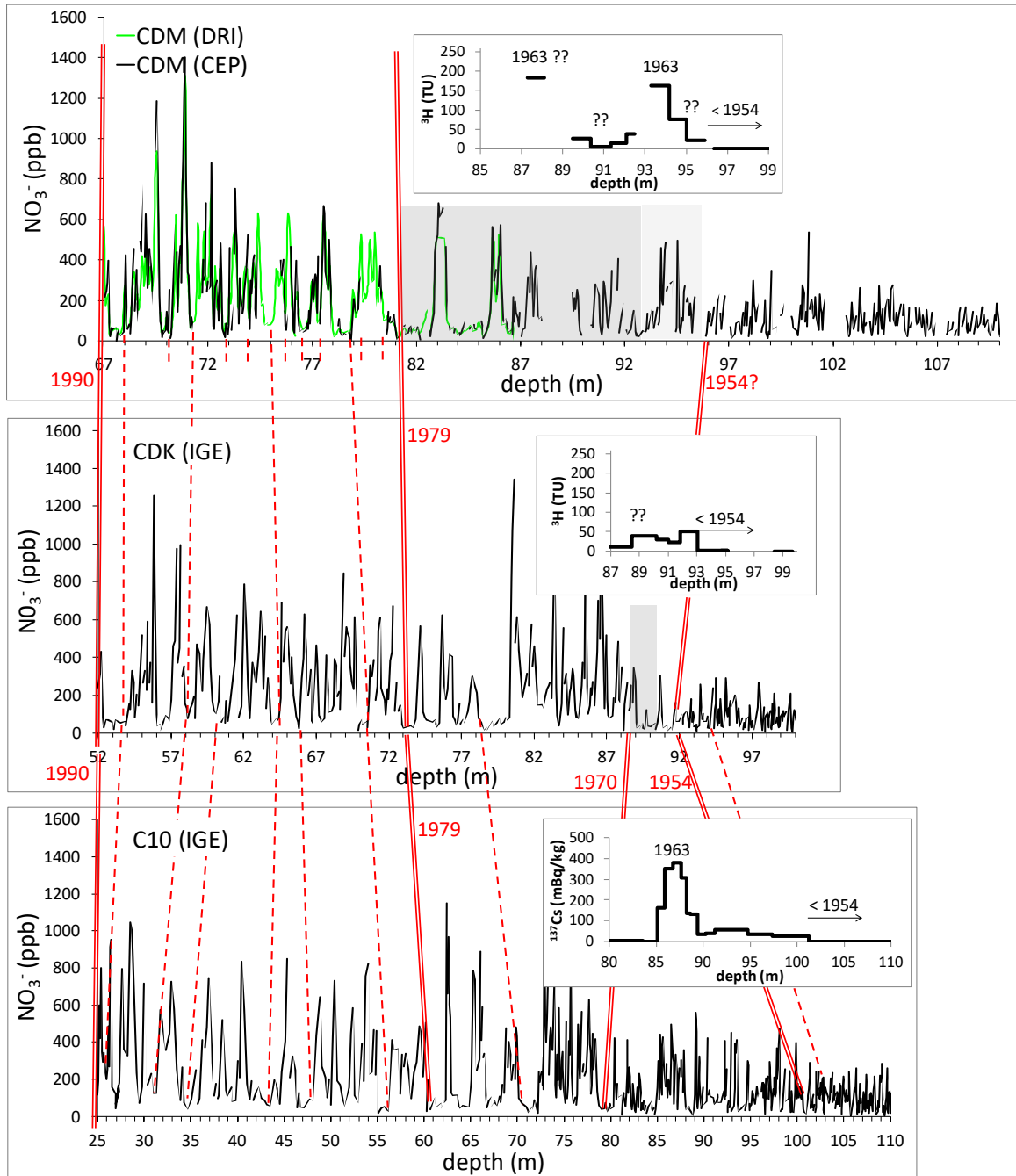
Figure 3. Comparison of nitrate depth stratigraphies of CDM (this study), CDK (Legrand et al., 2013) and C10 (Preunkert et al., 2003) ice. In addition, for each core the bomb test horizons also are reported (this study for CDM, Legrand et al., 2013 for CDK and Vincent et al., 1997 for C10). Red lines, complemented by annual layer marks in the upper undisturbed part of CDM, show common years in the different cores. Grey zones mark depth layers which do not fit in the continuous depth stratigraphies in CDM and CDK. Note that the chronological changes of the NO3 concentrations are offset in depth relative to each other due to the different years the cores were drilled.

with several outstanding atmospheric changes or events that occurred during the 20th century such as the ^{137}Cs peak caused by nuclear weapons testing fallout (Vincent et al. 1997), the well-marked increase of fluoride after 1930 resulting from the rapid growth of the aluminum industry (Preunkert et al., 2001b), the large increase of sulfate after World War II (Preunkert et al., 2001a), and hydrochloric acid (HCl) peaks during the hot summers from 1947 to 1949 caused by large forest fires (Legrand et al., 2002). Several of these events are recorded within the depth interval where increased ^{210}Pb values were observed (Vincent et al. 1997, Fig. 3 and Section 3.2). Thus, we can assume that the depth-age relation of the C10 core was not significantly disturbed (i.e., by more than the dating uncertainty estimated to be ± 5yr, at a depth of 90 m (Preunkert et al., 2000)) by the upstream crevasses which caused the anomaly of the ^{210}Pb record discussed in Section 3.2.

3.1.2 The CDK core

As done in the C10 core, the dating of the CDK ice core primarily was achieved by annual layer counting largely using the ammonium stratigraphy. However, the seasonality of ammonium as well as those of other major ions such as nitrate and sulfate disappears at 89.5 m and then recovers at 92 m (Legrand et al., 2013). Since the CDK ^{3}H profile lacks the main bomb maximum and ^{210}Pb anomalies were detected in this depth zone, Legrand et al. (2013) already concluded that net snow depositions of a few years around 1963 are missing due to the existence of upstream crevasses, but suggested neither a reasonable glaciological mechanism for this effect nor an explanation for whatever reason it appeared in CDK and not in C10. The comparison of ammonium, nitrate, and sulfate mean summer concentrations in the CDK core with those in C10 layers deposited above 89 m and between 92.0 and 106 m depth, however, suggests a reliable CDK record for the time intervals 2004-1970 and 1954-1925 (see Legrand et al., 2013 and Fig. 3 and 4).

3.1.3 The CDM core

Ionic species were analyzed as discrete samples using ion chromatography along the upper 35 m of the CDM core at IGE. From 45 m to 86 m depth, sections were measured using CFA at DRI (Legrand et al., 2018). These previous data were complemented by CFA measurements (NO_3^- and NH_4^+) performed at CEP. Figure 3 shows sequences of the CDM depth-profile for nitrate in comparison with those from CDK and C10. Down to 81 m depth, the nitrate CDM stratigraphy matches very well those from C10 and CDK, where this depth is dated to 1979 based on annual layer counting. Below 81 m depth, the CDM depth profile differs from those of the two other cores. The possibility that the three NO_3^- peaks between 81 and 88 m depth in the CDM core (Fig. 3) correspond to those seen between 73.2 and 78 m depth in CDK, would imply an annual layer thickness 1.75 times larger in the CDM than the CDK core. This conflicts with the expected decrease of annual layer thickness for strata having the same age in CDM compared to CDK drilled 8 years before. For instance, for the interval 1992-79 the annual layer thickness in CDM is approximately half that in CDK, as expected since the corresponding ice layers are deeper in the CDM core than in CDK (hence likely more thinned by glacier flow and having been deposited upstream further away from the drill site). In addition, the preceding assumption that the three nitrate peaks between 81 and 88 m depth in CDM date to 1978, 1977, and 1976, is in conflict with the ^{3}H level found in this core (see Fig. 3). Therefore, it is assumed that a

235   discontinuity occurs between 81 and at least 88 m depth in the CDM stratigraphy. Interestingly, whereas a winter to summer layer thickness ratio of ~0.55 is expected at ~80–100 m depth at this drill site, as seen in the C10 core (see Section 3 and Preunkert et al., 2000), a very high winter to summer layer contribution (>2) is observed in the CDM core between 81 and 88 m depth. Such an unexpectedly high winter to summer contribution was also observed in CDK between 89.5 and 92 m depth, i.e. where the NH_4^+ seasonal cycle vanished.

240
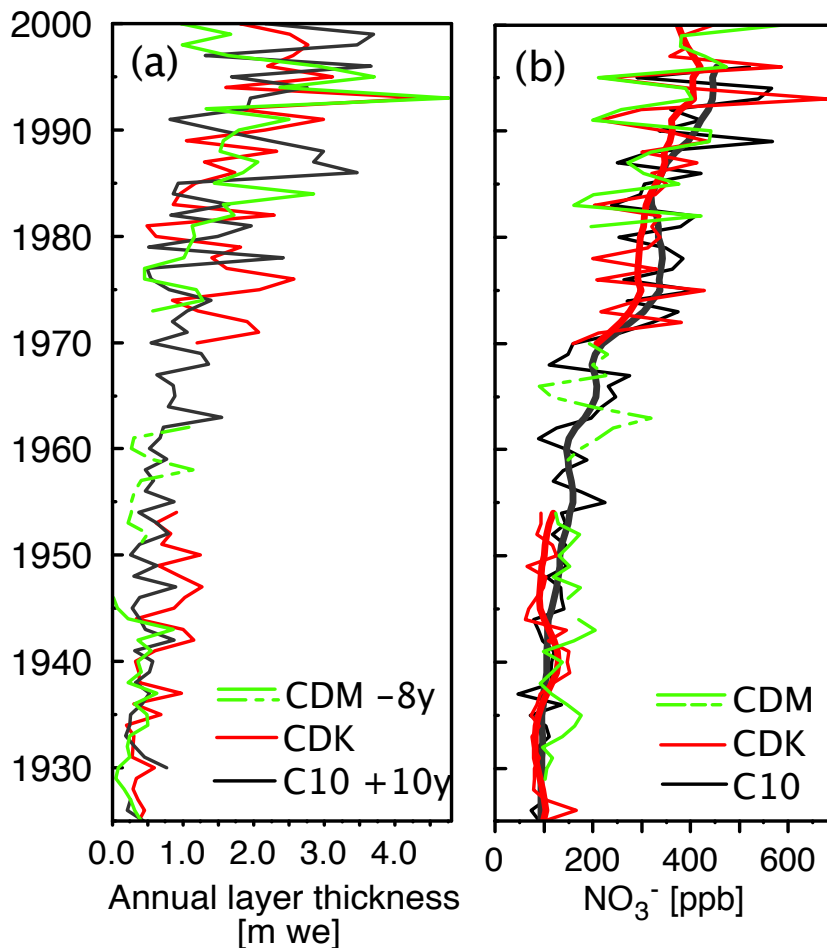
Figure 4: (a) Annual layer thickness of C10 (Preunkert et al. 2000) and CDK (Legrand et al., 2013) compared to CDM. To compensate for the different drilling dates of the three cores, annual layer thickness data of C10 and CDM were shifted for +10 and -8 years, respectively. For CDM, the annual layer thickness is estimated via the ammonium stratigraphy back to 1980 and via the
245   **nitrate (and ammonium) stratigraphy further back in time (Section 3.1.3). (b) comparison of nitrate summer half-year means of C10 (Preunkert et al., 2003), and CDK (Legrand et al., 2013) with CDM. The thick solid lines for C10 and CDK refer to the smoothed profile (single spectrum analysis, see Legrand et al., 2013). CDM depth intervals for which the dating is uncertain (Section 3.1.3), are marked with dashed lines.**

250   The inset in Fig. 3 (top panel) reports the ^3H profile measured on CDM ice core samples at CEP. Ages were assigned according to the expected ^3H concentrations based on comparison with values obtained in a high-resolution ice core from Fiescherhorn,

10

Switzerland (Schotterer et al. 1998). Strikingly, we find not one but two distinct peaks of 183.1 ± 9.7 TU and 162.7 ± 8.8 TU (one tritium unit, TU, being equal to 0.12 Bq L^{-1}) less than 6 m apart, starting at 87.29 to 88.2 m and 93.29 to 94.1 m depth, respectively. Both maxima are close to the ^{3}H peak value normally reached in 1963. Note that analytical or sample handling errors can be excluded since this anomaly has been confirmed by independent measurements made on different aliquots. Measurements on drill chips of the ice core from 87–88 m depth made at IUP indeed revealed 212 TU compared to 183.1 TU measured at CEP. Based on the undisturbed depth-age scale of core C10 drilled 18 years before CDM, the 1963 maximum would be expected at about 105 m depth in CDM (49 years before the 2012 drilling year). The ^{3}H profile of CDM, however, indicates low values below 96.3 m depth suggesting the ice is older than 1954. Referring to the disturbed depth-age relation in CDK, drilled 8 years before CDM, a 49-year-old ice layer should be located at 92 m depth, i.e., close to the second ^{3}H peak observed from 93.29 to 94.1 m depth in CDM. We therefore assume at this stage that the ^{3}H peak observed between 93.29 and 94.1 m depth in CDM ice corresponds to 1963.

Following what is expected from the Fiescherhorn depositional record, a mean TU value around the 1963 peak should be 10 to 40 TU in the years 1958-1975. This is consistent with the observed value in CDM ice around the second ^{3}H peak (89.5 to 96 m depth) except for the value of 6.4 TU observed at 90.3-91.3 m depth. Since the ^{3}H profile is available only at coarse resolution (75 cm long samples), it is not possible to be more accurate in dating the bomb test period (1954 to ~1976). Further arguments as to whether the ice layers around the ^{3}H peak in the CDM core (i.e. from 88-96 m depth) are well preserved were not conclusive. For example, if we assume that the profile is continuous between 93.3 and 96.3 m depth (i.e., 1954 as indicated by ^{3}H data) this would imply an annual layer thickness of 0.28 mwe over the 1963-1954 years, which is similar to what is seen in the C10 core (0.4 mwe). However, on the other hand, the NH_4^+ and NO_3^- depth stratigraphies from CDM do not agree with those in this part of C10. Because of decreasing anthropogenic emissions back in time, we consistently observed a decreasing trend in NH_4^+ and NO_3^- concentrations with age in the C10 ice (mean summer value in 1964–1968: NH_4^+: 110 ppb; NO_3^-: 178 ppb; in 1963–1954: NH_4^+: 95 ppb; NO_3^- 140 ppb). This feature, however, is not detected when comparing summer NH_4^+ and NO_3^- means in CDM ice above and below the 1963 peak at 93.3 m. Over the 88 to 93.3 m depth interval in CDM ice, we observed mean summer NH_4^+ and NO_3^- concentrations of 90 ppb and 175 ppb, respectively, which are lower than those between 93.3 and 96.3 m depth (NH_4^+: 116 ppb; NO_3^-: 193ppb; see also Fig. 4 for NO_3^-). Finally, annual layer counting based on the CDM nitrate or ammonium profiles suggests only 4 years instead of 9 years for the 93.3-96.3 m depth interval (i.e., from 1963 to 1954).

If the first ^{3}H peak is considered to be the true 1963 maximum, this would mean that a hiatus of 16 years exists in the CDM record between 1979 at 81 m depth and 1963 in 87.3 m depth. The depth layers between 88 and ~93.3 m depth would then correspond to years prior to 1963. This assumption is again in contradiction with the mean summer levels of NH_4^+ and NO_3^- observed in C10 for this period (see discussions above). Another stratigraphic perturbation is therefore required to produce the second ^{3}H maximum at 93.3 m.

In summary, our results suggest a continuous depth-age relation from the surface back to 1980 and for years older than ~1954 (96 m), implying a disturbed interval in between encompassing at least 25 years in this core. However, to confirm the assumption of the recovery of an undisturbed depth-age relation prior to 1954 done on the basis of the NO_3^- profile and the

observations made in C10 and CDK ice, further investigations of additional absolute time markers (as done in C10 ice, see Section 3.1) are needed before the lower part of the CDM core can be used as an archive of past atmospheric changes.

3.2 The ^{210}Pb depth profiles

Figure 5 reports the ^{210}Pb (half-life of 22.3 years) depth profiles of C10, CDK and CDM. ^{210}Pb is produced through radioactive decay from the noble gas ^{222}Rn (half-life of 3.8 days), which is an intermediate product in the normal radioactive decay chain of thorium and uranium, and emitted from the ground. ^{222}Rn is almost entirely produced from Radium in soils, in particular when granitic rocks are present. ^{222}Rn is released from soils into the atmosphere (Dörr and Münnich, 1990; Turekian et al., 1977), and its atmospheric sink consists in its radioactive decay producing ^{210}Pb, which becomes immediately attached to submicron aerosol particles (Whittlestone, 1990; Sanak et al., 1981).

Three common features can be identified in the ^{210}Pb depth profiles in each of the records. First, in the upper core Sections down to 80 m, the ^{210}Pb activities are of the order of magnitude of those expected from atmospheric deposition at high Alpine sites (Eichler et al., 2020; Gaeggeler et al., 2022). The fact that the expected decrease of ^{210}Pb activities by a factor of two over the 22 years (half life of ^{210}Pb) is not observed at the drill site is not surprising since the ^{210}Pb deposition at the glacier surface is not constant in time and space. Based on atmospheric ^{210}Pb measurements performed at high-elevation Alpine sites (see Hammer et al. (2007) for Sonnblick at 3106 m asl, Austria and Gaeggeler et al. (1995) for Jungfraujoch station at 3450 m asl, Switzerland), it was shown that the intensity of vertical upward transport of ^{210}Pb-rich continental boundary layer air masses strongly impacts ^{210}Pb levels at high elevation sites. As a consequence, a strong seasonal cycle with ^{210}Pb concentrations three to four times higher in summer than in winter is observed at high altitude Alpine sites. As expected, this also is observed in the snow deposition at CDD and shown in Fig S1a of the Supplement for summer 2004 and the outstanding hot summer 2003, for which an extremely enhanced upward transport was already reported previously (Legrand et al., 2005). Whereas in 2004 a summer to winter ^{210}Pb ratio of 2 was found, this ratio reached a factor of 7 in 2003. Together with the systematic decrease of the winter to summer layer thickness ratio with increasing core depth at the drill site (see Section 3 and Preunkert et al., 2000), this pronounced ^{210}Pb seasonality counteracts the expected ^{210}Pb decrease from radioactive decay.

Second, a well-marked anomaly characterized by ^{210}Pb enhancements (including ^{210}Pb peaks up to 10 times higher ^{210}Pb than expected from atmospheric deposition) is observed in the three cores. The anomaly extends from ~83 to 108 m depth (i.e., ~26 to 54 years) in C10, ~85 to 108 m (i.e., ~32 to 70 years) in CDK, and ~82 to 102 m (i.e., ~33 to more than 58 years) in CDM ice. The ^{210}Pb re-increase observed in CDK and CDM, however, is less pronounced than in C10. In addition, the starting depths of the CDK and CDM ^{210}Pb re-increases correspond to the 1970s, for which ^{210}Pb enhancements have been reported at other ice core sites (Eichler et al.,2000) and attributed to an enhanced vertical transport related to the temporal maximum of atmospheric sulfate aerosol acting as transport vehicle. To check whether these atmospheric conditions also could be responsible for the enhancement seen in CDK and CDM, we report exemplarily the CDK ^{210}Pb activity, corrected for its respective deposition date together with the corresponding sulfate concentration in Fig. S1b of the Supplement. As mentioned above, a strong seasonality was detected in the uppermost part of the CDK core for a few years where ^{210}Pb samples are

12

available in seasonal resolution (Fig. S1a of the Supplement). If atmospherically derived, mean ^{210}Pb concentrations of ice layers from 60 to 85 m depth (i.e., from 1988 to 1972), i.e., in the period for which the sulfate aerosol maximum was observed at CDD (Preunkert et al., 2001), would correspond to around 130 ± 60 mB kg^{-1}of ^{210}Pb in freshly deposited snow, which is comparable to the atmospherically derived ^{210}Pb further upward in the core. However, from 85 to 108 m depth, this connection

325   between sulfate levels and ^{210}Pb activity no longer holds. Whereas sulfate concentrations strongly decrease, ^{210}Pb at the time of deposition (decay-corrected) would be strongly enhanced (mean of 600 mBq kg^{-1}) and far above what is expected from atmospheric ^{210}Pb contributions. Thus, the mechanism proposed by Eichler et al. (2000) cannot be invoked in this part of the CDD core. For CDM (not shown) a similar picture appears. While from 80 to 90 m surface decay-corrected ^{210}Pb (160 ± 70 mBq kg^{-1}) would not have been significantly enhanced compared to the atmospherically derived ^{210}Pb concentrations seen

330   further up in the CDM core, this is not the case between 90 and 103 m depth. As for CDK, mean values at the time of deposition would have been around 650 mBq kg^{-1} and thus far too high to what would be expected from atmospheric transport.

Third, below the anomaly, a decrease in ^{210}Pb is observed. However, it is worth noting that, especially in the case of the CDM and CDK cores, ^{210}Pb activity (after blank correction) is above detection limits even in the bottommost core sections, while in C10 levels are below the detection limit. Since the age of the bottom core sections at CDD, however, exceeds several half-

335   lives of ^{210}Pb (as for example indicated by radiocarbon dating for CDK (Preunkert et al., 2019)) a zero ^{210}Pb activity is expected if the ^{210}Pb were only of atmospheric origin.

As mentioned above, we attribute the ^{210}Pb perturbations found at the drill site to the granite bedrock at CDD in combination with the presence of crevasses in the vicinity of the drill site. Pourchet et al. (2000) conducted measurements of ^{222}Rn in snow above a crevasse at the Mont Blanc summit, revealing unexpected peak values as high as 145,000 Bq m^{-3}, and free atmospheric

340   background values of a few tens of Bq m^{-3} at this elevation. Based on calculations, the authors suggested the existence of convective ^{222}Rn transport and diffusion from the underlying fractured granitic bedrock.

4. Discussion of upstream crevasse impact on ice core records

Since the ^{210}Pb anomalies are located at similar depths in C10, CDK and CDM cores (Section 3.2), and start in the three cores ~30 years before the drilling year, we assume that the ^{210}Pb perturbations originate from the same area upstream where one or

345   more crevasses reach bedrock. Furthermore, since the ^{210}Pb anomalies are restricted to a specific depth zone in the cores, we assume that exchange of the gaseous ^{222}Rn with the atmosphere is restricted or eliminated at the top by the presence of a snow-bridge containing horizontal summer ice layers such as have been observed to occur regularly at the site (Preunkert et al., 2000). Above the firn-ice transition of the glacier and below this snow-bridge, increased radiogenic Rn levels are then diffusing into the firn surrounding the closed-off crevasse (see Fig. 2b).

350
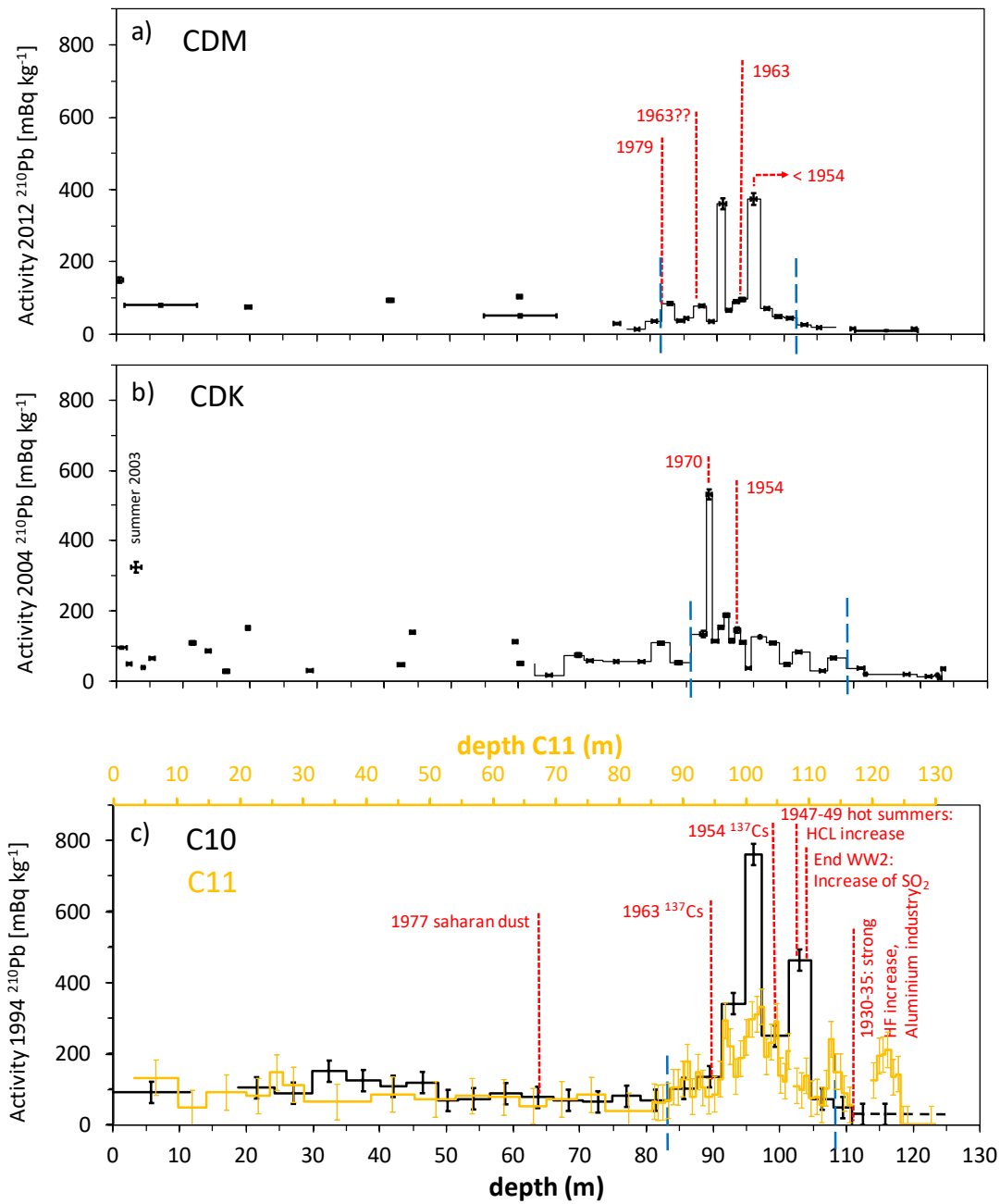
Figure 5: **210Pb profiles of the three CDD ice cores. The decay-corrected 210Pb activity is shown using the drilling year of the respective ice cores as reference.** For CDK (a) and CDM (b) the depths covered by the samples are plotted with thick black lines, whereas the thin integrating lines are given to guide the eye and were used to calculate the 210Pb inventories. C10 210Pb **data (c)** (lower x-axis, black) from Vincent et al. (1997) and this study are **compared to the ones of a 140 m long ice core extracted 30 m away from C10 in 1994 (Vincent et al., 1997, denoted here as C11, upper x-axis in c, orange). The depth scale of C11 was matched to achieve an overlay of the depths in 1963 and 1954 obtained from the respective 137Cs signals. Blue dashed vertical lines indicate the approximate boundaries of the anomaly. When available, absolute time markers detected over the 210Pb perturbed depth zones are also reported.**

14

360

The impact of the upstream crevasse on the depth-age relation of the ice cores changed, however, between the C10 core drilled in 1994 and the CDM and CDK cores drilled after 2000. Whereas for C10 an excellent agreement between annual layer counting and independent absolute time markers was found over the depth interval influenced by the crevasse, i.e. in which increased ^{210}Pb values were observed (Fig. 5), this is not the case for the CDK and CDM ice cores. In the latter two cores, the

365 ^{210}Pb anomaly comprises the layers for which the depth-age relation was found to be disturbed (see Section 3 and Fig. 3 and 5). Furthermore, the CDK and CDM ^{210}Pb anomaly inventories (Fig. 5) are 4 times lower than in C10, whereas we would have expected similar ^{210}Pb anomaly inventories if the bedrock surface of the crevasse and its surrounding ice layer stratigraphy had remained unchanged. The spatial variability of the ^{210}Pb anomaly inventory at the CDD site can be estimated by examining the ^{210}Pb inventory of a 140 m long ice core extracted in 1994 almost at the low point of the Col du Dome saddle ~ 30 m south-

370 east from C10 (Vincent et al., 1997 and see Fig. 5c). This core revealed a ^{210}Pb anomaly inventory of 80% of that in C10. Hence, although this 1994 core does not have the same upstream ice flow characteristics as the 3 cores examined here because of its different position and length, this difference is small compared to the difference seen between C10, CDK, and CDM. Thus, the two preceding points suggest that the upstream glacier flow of the drill site in the area of the crevasse has changed with time.

375 Tracing back the arrival depths of the ^{210}Pb disturbance at the drill site, model calculations made by Vincent et al. (1997) (not shown) and Gilbert et al. (2014) (Fig. 2a, b and c) suggest that the origin of the ^{210}Pb anomaly should lie ~100-150 m upstream of the drill site, which is in good agreement with visual observations of the crevasse obtained via aerial and ground-based photos (see Fig. 2b and c, and Fig. 1). A bedrock reaching crevasse (see Fig. 2b) capped by snow and ice layers at the top which is situated near or within the upstream flowline would lead to a continuous enrichment of ^{222}Rn and ^{210}Pb within the air

380 volume of the crevasse itself, and by diffusion or barometric pumping (Birner et al., 2018) of ^{222}Rn into the firn surrounding the open part of the crevasse (see the shaded areas in Fig. 2b and c). As mentioned above, the ^{222}Rn diffusion would be sealed by the presence of a snow-bridge containing impermeable ice layers at the top (see dotted area in Fig. 2b and c) and the firn-ice transition of the glacier at the bottom, respectively. This would imply that the firn ice transition lies at a depth of ~50 m (i.e. ~20 years) in the surrounding area of the crevasse (see Fig. 2b), whereas the observed firn ice transition is located at ~25

385 m depth at the summit of Dome de Gouter (i.e., ~100 years, Rehfeld, 2009) and at ~50-55 m depth at the C10, CDK and CDM drill site (i.e., ~13-14 years). After having been enriched in ^{210}Pb, the firn/ice layers would continue to flow downslope and thereafter arrive at the drill site as indicated by the bold green flow lines in Fig. 2b. A rough estimation for the transit time between the crevasse and the drill site can be done following the flow lines of the ice flow model of Gilbert et al. 2014 (see Fig. 2b). Doing so, 30-year-old ice found at a depth of ~80 m depth at the CDD drill site would have passed nearby or crossed

390 the crevasse ~25 years before.

Although speculative, we assume that the upstream crevasse of Fig. 1 and 2 already existed earlier in the 1970s but was limited in its width and/or horizontal extension. If either the crevasse did not intersect the catchment area of the drill site or the crevasse was so narrow, that even intersecting the catchment area of the drill site, the chronology of the C10 ice core was not disturbed,

this would explain the occurrence of the ^{210}Pb anomaly observed in C10 together with an undisturbed depth-age relation in.

395 For this hypothesis to hold we assume that a crevasse capped at the top. In this case the enhanced ^{222}Rn levels in the capped crevasse entered the firn layers adjacent to the crevasse leading to elevated ^{210}Pb inventories, which then flowed down to the C10 location. In contrast, the crevasse later extended into the upstream flow line of cores CKK and CDM, thus not only elevating the ^{210}Pb levels but also disturbing the chronologies. Assuming that the crevasse would have enlarged and also propagated horizontally to definitely cross the flow line of the drill site, the appearances of winter snow enriched layers and

400 discontinuities (i.e. lacking and/or doubling of ice layers) in the depth-age relations of CDK and CDM, drilled 10 and 18 years later than C10, can be explained. The presence of unexpectedly large winter snow layers observed in CDK and CDM (Section 3.1.3) can then be attributed to the disintegration of the snow bridge or directly to blowing winter snow filling the crevasse. The lack of or the doubling of ice layers can be explained by a shift in the isochrones occurring from the ice layer transition through the crevasse (or crevasse system).

405 For the ice layer transition through the crevasse, two scenarios could be imaginable. Due to the bedrock and glacier surface inclination, ice of the upstream wall of the crevasse (left side of the crevasse in Fig. 2c) would be mapped offset to the downstream wall of the crevasse (right side of the crevasse in Fig. 2c) in the sense that an upstream isochrone arrives at a deeper depth compared to this isochrone on the downstream side of the crevasse (see pink arrow in Fig. 2c). This would result in a layer doubling at the drill site after the inflow of the isochrones into the ice core drill site, as it is seen in CDM. On the

410 other hand, if the bottom of the crevasse is filled up with snow from the previously existing snow bridge and/or from wind-blown surface snow, it might happen that isochrones of the upstream wall of the crevasse arrive at shallower depths compared to the respective isochrones on the downstream wall of the crevasse (see orange arrow in Fig. 2c). This would result in missing layers at the drill site as seen in CDK.

We stress that although a decay-corrected ^{210}Pb anomaly is visible in all three cores, the anomalies in the CDM and CDK cores

415 are smaller than in C10. This could be explained by a (temporary?) opening of the crevasse to the atmosphere. A partial opening of the crevasse to the atmosphere would allow the bedrock-derived ^{222}Rn in the crevasse to mix with the much lower atmospheric ^{222}Rn concentrations (Pourchet et al., 2000). This would have led to a strong reduction of additional ^{222}Rn accumulation and ^{210}Pb production in the crevasse and in the snow and firn around the crevasse, starting from the moment of the opening to the atmosphere. This would explain ^{210}Pb inventories of 70 and 55% in CDK and CDM compared to C10,

420 because of the radioactive decay of ^{210}Pb accumulated before the opening of the crevasse to the atmosphere, over 10 and 18 years, respectively. However, the measured ^{210}Pb anomaly inventories of CDK and CDM cores amount to only ~25% of the C10 inventory. This suggests that in addition to the opening of the crevasse the isochrones in the CDK and CDM cores are disturbed, leading to a lack of ice layers with high ^{210}Pb activities.

Interestingly, although recent long-term glaciological observations of the CDD site are only available since 1994 and show

425 only minor changes in glacier dynamics (Vincent et al., 2020), a glacier thickness reduction of ~6-7m, being the maximal value of the whole saddle area, was observed from 1994 to 2017 in the crevasse area upstream of the C10, CDK, and CDM drill sites (Fig. 2a). This could be a sign of a partly collapsing crevasse, that could lead to further stratigraphic disruptions (compared to CDM and CDK) at the drill site in the future.

5. Summary and conclusion

Combining existing and new chemical depth profiles, bomb test time markers, and the ^{210}Pb depth profiles of three ice cores extracted at the same drill CDD site in 1994, 2004 and 2012, allowed us for the first time to highlight changes over time in the depth-age characteristics at an alpine drill site. Because of the granitic bedrock prevailing at the site, the imprint of a crevasse located upstream of the drill site is visible in all three ice cores, as a distinct anomaly in their ^{210}Pb profiles extending over just a few meters in depth and with ^{210}Pb concentrations elevated by up to a factor of 10. Whereas the depth-age relation of the C10 ice core drilled in 1994 does not appear to be disturbed by the crevasse in the upstream region, this is not the case for the CDK and CDM ice cores drilled after 1994 (in 2004 and 2012). For CDK and CDM, the depth-age relationships were found to be disturbed in ice layers deposited ~30 year before drilling and over a period of 16 years in CDK and at least 25 years in CDM and we attribute this to an extension of the crevasse over time into the upstream flowline of our drill site. This finding is consistent with long-term glaciological observations that show significant glacier thickness changes in the area surrounding the upstream crevasse.

Although at this stage we can provide only a qualitative explanation for the recently observed stratigraphic discontinuities, our work points towards the need for careful examination of depth-age relationships, when using ice cores from this CDD drill site, to reconstruct past atmospheric conditions. More generally, since crevasses are often present on non-polar glaciers, such disturbances in the depth-age relation, as observed at CDD, could also appear at other non-polar ice core drill sites but may be undetected; particularly, when the bedrock is not granitic, when few or no absolute time markers are available, and/or when only one core is collected from the site. To identify such depth-age problems, in addition to the commonly used annual layer counting, an extended use of absolute time markers including bomb horizons through ^{3}H, ^{137}Cs, or [239]Pu (Arienzo et al., 2016), [39]Ar (Feng et al., 2019), large Saharan dust events or volcanoes (e.g., Plunkett et al., 2022) is mandatory. Furthermore, at other non-polar sites where the net snow accumulation is far lower than at CDD (i.e., with ice as old as several thousands of years located well above the bedrock), additional tools like ^{14}C measurements (Jenk et al., 2006 and 2009; Hoffmann et al., 2018) should be applied.

Data availability

Ice core data are available at NCEI (National Centers for Environmental Information) data base (https://www.ncei.noaa.gov/access/paleo-search/study/38020).

Author contribution

Acknowledgements

Competing interests

The authors declare that they have no conflict of interest.

References

Arienzo, M.M., Legrand, M., Preunkert, S., Stohl, A., Chellman, N., Eckhardt, S., Gleason, K.E. and McConnell J.R.: Alpine ice-core evidence of a large increase in vanadium and molybdenum pollution in Western Europe during the 20th century. Journal of Geophysical Research: Atmospheres, 126, e2020JD033211, https://doi.org/10.1029/2020JD033211, 2021.

Arienzo, M.M., McConnell, J.R., Chellman, N. Criscitiello, A., Curran, M., Fritzsche, D., Kipfstuhl, S., Mulvaney, R., Nolan, M. Opel, T. Sigl, M. and Steffensen, J.P.: A method for continuous ^{239}Pu determinations in Arctic & Antarctic ice cores, *Environ Sci Technol,* doi: 10.1021/acs.est.6b01108, 2016.

Birner, B., Buizert, C., Wagner, T.J.W. and Severinghaus, J.P.: The influence of layering and barometric pumping on firn air transport in a 2-D model. The Cryosphere 12, 2021-2037, https://doi.org:10.5194/tc-12-2021-2018, 2018.

Bohleber, P.: Alpine Ice Cores as Climate and Environmental Archives, https://doi.org/10.1093/acrefore/9780190228620.013.743, 2019.

Colgan, W., Rajaram, H., Abdalati, W., McCutchan, C., Mottram, R., Moussavi, M., and Grigsby, S.: Glacier Crevasses: Observations, Models and Mass Balance Implications. Rev. Geophys., 54, 119-161, https://doi.org/10.1002/2015RG000504, 2016.

Dörr, H., and Münnich, K. O.: ^{222}Rn flux and soil air concentration profiles in West Germany. Soil Rn as tracer for gas transport in the unsaturated soil zone, Tellus, Ser. B, 42, 20–28, https://doi.org/10.1034/j.1600-0889.1990.t01-1-00003.x, 1990.

Eichler, A., Schwikowski, M., Gäggeler, H. W., Furrer, V., Synal, H. A., Beer, J., and Funk, M.: Glaciochemical dating of an ice core from upper Grenzgletscher (4200 m a.s.l.). Journal of Glaciology, 46(154), 507-515, https://doi.org/10.3189/172756500781833098, 2000.

Eichler, A., Legrand, M., Jenk, T. M., Preunkert, S., Andersson, C., Eckhardt, S. Engardt, M. Plach, A. and Schwikowski, M.: Consistent histories of anthropogenic Western European air pollution preserved in different Alpine ice cores, The Cryosphere, https://doi.org/10.5194/tc-2022-208, 2023.

Elsässer, C., Wagenbach, D., Weller, R., Auer, M., Wallner, A., and Christl, M.: Continuous 25-yr aerosol records at coastal Antarctica Part 2: variability of the radionuclides ^{7}Be, ^{10}Be and ^{210}Pb, Tellus B, 63(5), 920-934,

19

https://doi.org/10.1111/j.1600-0889.2011.00543.x, 2011.

515   Erhardt, T., Bigler, M., Federer, U., Gfeller, G., Leuenberger, D., Stowasser, O. et al., High-resolution aerosol concentration
        data from the Greenland NorthGRIP and NEEM deep ice cores. Earth System Science Data, 14(3), 1215-1231,
        https://doi.org/10.5194/essd-14-1215-2022, 2022.

        Fagerli, H., Legrand, M., Preunkert, S., Vestreng, V., Simpson, D., and Cerqueira, M.: Modeling historical long-term trends
520   of sulfate, ammonium, and elemental carbon over Europe: A comparison with ice core records in the Alps, J. Geophys. Res.,
        112, D23S13, https://doi.org/10.1029/2006JD008044, 2007.

        Feng Z., Bohleber, P., Ebser S., Ringena L., Schmidt, M., Kersting A., Hopkin P., Hoffmann, H., Fischer A., Aeschbach W.,
        and Oberthaler M.K.: Dating glacier ice of the last millennium by quantum technology, Proc. Natl. Acad. Sci. U.S.A. 116,
525   8781–8786, https://doi.org/10.1073/pnas.1816468116, 2019.

        Gäggeler HW; Radioactivity in the Atmosphere, Radiochimica Acta 70/71, 345-35,
        https://doi.org/10.1524/ract.1995.7071.s1.345, 1995.

530   Gäggeler, H., Tobler, L., Schwikowski, M., and Jenk, T.: Application of the radionuclide 210 Pb in glaciology – an
        overview, Journal of Glaciology. 66. 1-10, https://doi.org/10.1017/jog.2020.19 , 2020.

        Gfeller, G., Fischer, H., Bigler, M., Schüpbach, S., Leuenberger, D., and Mini, O.: Representativeness and seasonality of major
        ion records derived from NEEM firn cores, The Cryosphere, 8, 1855–1870, https://doi.org/10.5194/tc-8-1855-2014 , 2014.
535
        Gilbert, A. and Vincent, C.: Atmospheric temperature changes over the 20th century at very high elevations in the European
        Alps from englacial temperatures, Geophysical Research Letters, 40, 2102–2108, https://doi.org/10.1002/grl.50401, 2013.

        Gilbert, A., Gagliardini, O., Vincent, C., and Wagnon, P.: A 3-D thermal regime model suitable for cold accumulation zones
540   of   polythermal   mountain   glaciers,   Journal   of   Geophysical   Research: Earth   Surface,   119(9),   1876-1893,
        https://doi.org/10.1002/2014JF003199, 2014.

        Guilhermet, J., Preunkert, S., Voisin, D., Baduel, C., and Legrand, M.: Major 20th century changes of water-soluble HUmic
        LIke Substances (HULISWS) aerosol over Europe inferred from Alpine ice cores, J. Geophys. Res. Atmos., 118,
545   https://doi.org/10.1002/jgrd.50201, 2013.

        Hammer, S., Wagenbach, D., Preunkert, S., Pio, C., Schlosser, C., and Meinhardt, F.: Lead-210 observations within

CARBOSOL: A diagnostic tool for assessing the spatiotemporal variability of related chemical aerosol species?, J. Geophys. Res., 112, D23S03, https://doi.org/10.1029/2006JD008065, 2007.

550

Hoffmann, H., Preunkert, S., Legrand, M., Leinfelder, D., Bohleber, P., Friedrich, R., and Wagenbach, D.:, A new sample preparation system for micro-14C dating of glacier ice with a first application to a high alpine ice core from Colle Gnifetti (Switzerland), Radiocarbon, 60(02), 517–533, https://doi.org/10.1017/rdc.2017.99, 2018.

555 Jenk, T., Szidat, S., Schwikowski, M., Gäggeler, H., Brütsch, S., Wacker, L., Synal, H.-A., and Saurer, M.: Radiocarbon analysis in an alpine ice core: Record of anthropogenic and biogenic contributions to carbonaceous aerosols in the past (1650– 1940). Atmospheric Chemistry and Physics, 6(12), 5381–5390, https://doi.org/10.5194/acp-6-5381-2006 , 2006.

Jenk, T., Szidat, S., Bolius, D., Sigl, M., Gäggeler, H., Wacker, L, Ruff, M., Barbante, C., Boutron, C.F., Schwikowski, M.: A 560 novel radiocarbon dating technique applied to an ice core from the Alps indicating late Pleistocene ages, Journal of Geophysical Research, 114, D14305. https://doi.org/10.1029/2009JD011860, 2009.

Kaufmann; P.R., Federer, U., Hutterli, M.A., Bigler, M., Schüpbach, S., Ruth, U., Schmitt, J., and Stocker, T.F.: An improved Continuous Flow Analysis (CFA) system for high-resolution field measurements on ice cores, Environ. Sci. 565 Technol., 42, 21, 8044–8050, https://doi.org/10.1021/es8007722, 2008.

Legrand, M., de Angelis, M., and Delmas, R. J.: Ion chromatographic determination of common ions at ultratrace levels in Antarctic snow and ice, Anal. Chim. Acta, 156, 181-192, https://doi.org/10.1016/S0003-2670(00)85549-X, 1984.

570 Legrand, M., Preunkert, S., Wagenbach, D., and Fischer, H.: Seasonally resolved Alpine and Greenland ice core records of anthropogenic HCl Emissions over the 20th century, J. Geophys. Res., 107, D12, https://doi.org/10.1029/2001JD001165, 2002.

Legrand, M., Preunkert, S., Wagenbach, D., Cachier, H., and Puxbaum, H.: A historical record of formate and acetate from a 575 high elevation Alpine glacier: Implications for their natural versus anthropogenic budgets at the European scale, J. Geophys. Res., 108, D24, 4788, https://doi.org/10.1029/2003JD003594, 2003.

Legrand, M., Preunkert, S., Galy_Lacaux, C., Liousse, C., and Wagenbach, D., Atmospheric year-round records of dicarboxylic acids and sulfate at three French sites located between 630 and 4360 m elevation, J. Geophys. Res., 110, 580 doi:10.1029/2004JD005515, 2005.

Legrand, M., Preunkert, S., Schock, M., Cerqueira, M., Kasper-Giebl, A., Afonso, J., Pio, C., Gelencsér, A., and Dombrowski-

Etchevers, I.: Major 20th century changes of carbonaceous aerosol components (EC, WinOC, DOC, HULIS, carboxylic acids, and cellulose) derived from Alpine ice cores, J. Geophys. Res., 112, D23S11, https://doi.org/10.1029/2006JD008080 , 2007.

585

Legrand, M., Preunkert, S., May, B., Guilhermet, J., Hoffman, H., and Wagenbach, D.: Major 20th century changes of the content and chemical speciation of organic carbon archived in Alpine ice cores: Implications for the long-term change of organic aerosol over Europe, J. Geophys. Res, 118(9), 3879-3890, https://doi.org/10.1002/jgrd.50202 , 2013.

590   Legrand, M., McConnell, J. R., Preunkert, S., Arienzo, M., Chellman, N., Gleason, K., Sherwen, T., Evans, M. J., and Carpenter, L. J., Alpine ice evidence of a three-fold increase in atmospheric iodine deposition since 1950 in Europe due to increasing oceanic emissions, Proceedings of the Nat. Academy of Sciences of the USA, https://doi.org/10.1073/pnas.1809867115, 2018.

595   Legrand, M., McConnell, J. R., Lestel, L., Preunkert, S., Arienzo, M., Chellman, N. J., Stohl, A., Eckhardt, S.: Cadmium pollution from zinc-smelters up to fourfold higher than expected in western Europe in the 1980s as revealed by alpine ice. Geophysical Research Letters, 46, e2020GL087537, https://doi.org/10.1029/2020GL087537, 2020.

Legrand, M., McConnell, J. R., Preunkert, S., Chellman, N. J., and Arienzo, M. M.: Causes of enhanced bromine levels in
600   Alpine ice cores during the 20th century: Implications for bromine in the free European troposphere, J. Geophys. Res, 126, e2020JD034246, https://doi.org/10.1029/2020JD034246, 2021.

Legrand, M., McConnell, J. R., Preunkert, S., Bergametti, G., Chellman, N. J., Desboeufs, K., Plach, A., Stohl, A., Eckhardt, S.: Thallium pollution in Europe over the twentieth century recorded in Alpine ice: Contributions from coal burning and
605   cement production. Geophysical Research Letters, 49, e2022GL098688, https://doi.org/10.1029/2022GL098688, 2022.

Moseid, K. O., Schulz, M., Eichler, A., Schwikowski, M., McConnell, J. R., Olivié, D., Criscitiello, A. S., Kreutz, K.J., and Legrand, M.: Using ice cores to evaluate CMIP6 aerosol concentrations over the historical era. J. Geophys. Res., 127, e2021JD036105, https://doi.org/10.1029/2021JD036105, 2022.

610

Pinglot, JF, and Pourchet, M.: Radioactivity measurements applied to glaciers and lake sediments, Sci. of the Tot. Env., 173-174, 211-233, https://doi.org/10.1016/0048-9697(95)04779-4, 1995.

Pinglot, J. F. , Vaikmae, R. , Kamiyama, K. , Igarashi, M. , Fritzsche, D. , Wilhelms, F. , Koerner, R. , Henderson, L. ,
615   Isaksson, E. , Winther, J. G. , van de Wahl, R. S. W. , Fournier, M. , Bouisset, P. and Meijer, H. A. J.: Ice cores from Arctic sub-polar glaciers: chronology and post-depositional processes deduced from radioactivity measurements , Journal of Glaciology, 49 (164), 149-158, https://doi.org/10.3189/172756503781830944, 2003.

Plunkett, G., Sigl, M., Schwaiger, H., Tomlinson, E., Toohey, M., Mcconnell, J., Pilcher, J., Hasegawa, T., and Siebe, C.: No

620   evidence for tephra in Greenland from the historic eruption of Vesuvius in 79 CE: Implications for geochronology and

paleoclimatology, Climate of the Past, https://doi.org/10.5194/cp-2021-63, 2000.

Pourchet, M, Richon, P.,, Sabroux, J.-C.: Lead-210 and radon-222 anomalies in Mont Blanc snow, French Alps. Journal of

Environmental Radioactivity. 48. 349–357, https://doi.org/10.1016/S0265-931X(99)00084-3, 2000.

625

Preunkert, S., Wagenbach, D., Legrand, M., and Vincent, C.: Col du Dôme (Mt Blanc Massif, French Alps) suitability for ice-

core studies in relation with past atmospheric chemistry over Europe. Tellus B, 52(3), 993-1012,

https://doi.org/10.3402/tellusb.v52i3.17081, 2000.

630   Preunkert, S., Legrand, M., and Wagenbach, D.: Sulfate Trends in a Col du Dôme (French Alps) Ice Core: A Record of

Anthropogenic Sulfate Levels in the European Mid-Troposphere over the 20th Century, J. Geophys. Res., 106, 31991-32004,

https://doi.org/10.1029/2001JD000792, 2001a.

Preunkert, S., Legrand, M., and Wagenbach, D.: Causes of enhanced fluoride levels in Alpine ice cores over the last 75 years:

635   Implications   for   the   atmospheric   fluoride   budget,   J.   Geophys.   Res,   106(D12),   12619-12632,

https://doi.org/10.1029/2000JD900755, 2001b.

Preunkert, S., Wagenbach, D., and Legrand, M.: A seasonally resolved Alpine ice core Record of Nitrate: Comparison with

Anthropogenic Inventories and estimation of Pre-Industrial Emissions of NO from Europe, J. Geophys. Res., 108, D21, 4681,

640   https://doi.org/10.1029/2003JD003475, 2003.

Preunkert, S., McConnell, J. R., Hoffmann, H., Legrand, M., Wilson, A. I., Eckhardt, S., Stohl, A., Chellman, N., Arienzo,

M., and Friedrich, R.: Lead and antimony in basal ice from Col du Dome (French Alps) dated with radiocarbon: A record of

pollution during antiquity, Geophys. Res. Lett., 46, 4953-4961, https://doi.org/10.1029/2019GL082641, 2019.

645

Rehfeld, K.: Investigations into Mont Blanc region summit ice cores at seasonal resolution, Institute of Environmental Physics,

Diploma thesis, University of Heidelberg, Germany, 2009.

Sanak, J., Gaudry, A. and Lambert, G.: Size distribution of Pb-210 aerosols over oceans, Geophys. Res. Lett., 8(10), 1067–

650   1069, https://doi.org/10.1029/GL008i010p01067, 1981.

Schotterer, U., Schwarz, P., and Rajner, V.: From pre-bomb levels to industrial times: A complete tritium record from an alpine

ice core and its relevance for environmental studies. In Isotope techniques in the study of environmental change, International Atomic Energy Agency (IAEA), 1998.

655

Stanzick, A.: Raum-Zeit-Variationen von Be-10, Pb-210 und Cl-36 in der grönländischen Firndecke: Luft-Firn-Transfer und rezente Trends, PhD thesis, Institute of Environmental Physics, University of Heidelberg, Germany, 2001.

Turekian, K. K., Nozaki, Y., and Benninger, L. K.: Geochemistry of atmospheric radon and radon products, Annu. Rev.

660 Earth Planet. Sci., 5, 227 – 255, https://doi.org/10.1146/annurev.ea.05.050177.001303, 1977.

Vimeux, F., Angelis, M., Ginot, P., Magand, O., Casassa, G., Pouyaud, B., Falourd, S., Johnsen, S.: A promising location in Patagonia for paleoclimate and paleoenvironmental reconstructions revealed by a shallow firn core from Monte San Valentín (Northern Patagonia Icefield, Chile). J. Geophys. Res. 113. 10.1029/2007JD009502, 2008.

665

Vincent, C., Vallon, M., Pinglot, J. F., Reynaud, L., and Funk, M.:, Snow accumulation and ice flow at Dôme du Goûter (4300 m), Mont Blanc, French Alps, Journal of Glaciology, 43(145), 513-521, https://doi.org/10.3189/S0022143000035127, 1997.

Vincent, C., Le Meur, E., Six, D., Possenti, P., Lefebvre, E., and Funk, M.: Climate warming revealed by englacial

670 temperatures at Col du Dôme (4250 m, Mont Blanc area), Geophys. Res. Lett., 34, L16502, https://doi.org/10.1029/2007GL029933, 2007.

Vincent, C., Gilbert, A., Jourdain, B., Piard, L., Ginot, P., Mikhalenko, V., Possenti, P., Le Meur, E., Laarman, O. and Six, D.: Strong changes in englacial temperatures despite insignificant changes in ice thickness at Dôme du Goûter glacier (Mont Blanc

675 area), The Cryosphere, 14. 925–934, https://doi.org/10.5194/tc-14-925-2020, 2020.

Wagenbach, D., Bohleber, P., and Preunkert, S.: Cold, alpine ice bodies revisited: what may we learn from their impurity and isotope content?, Geografiska Annaler: Series A, Physical Geography, 94(2), 245-263, https://doi.org/10.1111/j.1468-0459.2012.00461.x, 2012.

680

Whittlestone, S.: Radon daughter disequilibria in the lower marine boundary layer, J. Atmos. Chem., 11, 27–42, https://doi.org/10.1007/BF00053666, 1990.